High power reflector simulation to optimize electrical energy consumption and temperature profile

Kourosh Mousavi Takami, Örjan Danielsson, Jafar Mahmoudi

Accepted Manuscript

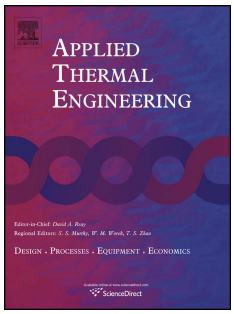

Title: High power reflector simulation to optimize electrical energy consumption and temperature profile

Authors: Kourosh Mousavi Takami, Örjan Danielsson, Jafar Mahmoudi

PII: S1359-4311(10)00427-8

DOI: 10.1016/j.applthermaleng.2010.09.031

Reference: ATE 3258

To appear in: *Applied Thermal Engineering*

Received Date: 31 May 2010

Revised Date: 30 September 2010

Accepted Date: 30 September 2010

Please cite this article as: K.M. Takami, Ö. Danielsson, J. Mahmoudi. High power reflector simulation to optimize electrical energy consumption and temperature profile, Applied Thermal Engineering (2010), doi: 10.1016/j.applthermaleng.2010.09.031

High power reflector simulation to optimize electrical energy consumption and temperature profile

Kourosh Mousavi Takami[1], Örjan Danielsson[2], and Jafar Mahmoudi[3]

[1,3] Mälardalen University, Box 883, SE 72123, Västerås, Sweden; Tel: +46 700 727 156, Fax: +46 21 101370 [2] Kanthal AB, Box 502, SE – 734 27 Hallstahammar, Sweden

Korosh_sari@yahoo.com, kourosh.mousavi.takami@mdh.se; orjan.danielsson@kanthal.com; jafar.mahmoudi@mdh.se

Abstract: The high power reflector is a new heating solution for use in high power heating systems. It consists of a vacuum formed ceramic fibre hood with an integrated Kanthal® Super ceramic heating element. This paper describes simulations that have been performed to optimise characteristics of the high power reflector with respect to output heat power and temperature distribution. The main motivation for this task is to use this system in the annealing furnaces of Surahammar Bruks AB. Simulations of heat transfer were performed with different reflector configurations in the COMSOL® software environment. We examined six different types of proposed reflector using a two dimensional model approach. The temperature variations with distance above the reflectors and the temperature profiles in surfaces 20 cm above the elements were simulated. Optimum shapes and dimensions were found that produced the highest peak temperature, mean temperature, and uniform temperature distribution in the surface above the element. 3D simulations were performed to verify the accuracy of the 2D simulations. The maximum difference between the 2D and 3D results was about 5%. The results showed a satisfactory fit with average furnace temperatures.

I. INTRODUCTION

High power reflectors are used in a wide range of metal industries. The two main parts of this high temperature heater system are the electrical heating element and the insulating fibre hood. This type of heater is very efficient due to its fast warm up and cooling. The high operating temperatures, high

performance in many industrial applications, competitive price, long life, easy installation and maintenance and the benefits to the environment as a result of their ability to run on clean energy are among the advantages of high power reflectors. This type of high temperature heater can be used in melting furnaces for materials like aluminium and glasses, annealing furnaces for strip rolling processes, laboratory furnaces, deformation industries and many other applications.

The reflector is made of ceramic fibre or other appropriate materials that can withstand the high temperatures in question.

The electrical resistor elements of this system are of the well known molybdenum silicide type. This type of heating element is widely used in industry. It can be used at higher operating temperatures than silicon carbide heating elements, and is primarily intended for use in high temperature applications, mostly in conjunction with furnaces and ovens, which operate at temperatures of around 1700°C.

The main producers of molybdenum silicide electrical heating elements are Kanthal AB [1], I Squared R Element Co. Inc. [2], Rotfil s.r.l. [3] and Duralite Inc. [4].

Optimization of energy consumption and loss reduction in industries can increase the efficiency and yield of power equipment. Customers look for high efficiency along with uniform temperature distribution on the work surfaces in furnace or melting devices. In order to achieve this, it is necessary to minimize the heat losses in the heating elements in high power reflectors and to optimize the heating performance relative to output power and temperature distribution. This can be done by altering the size and shape of the heating element and the insulating ceramic fibre to reflect as much power as possible from the module.

The Superthal® high power reflector (shown in Figure 1) is a compact fibre insulated modular heater with integrated Kanthal Super elements. It is designed to produce up to 110 kW/m^2 at 1650°C [5]. Its technical specifications are presented in Table 1.

The Superthal high power reflector can be used wherever concentrated high power is needed at temperatures up to 1650°C, such as in single billet heating, aluminium melting furnaces or ladle heaters [5].

The main objective of the studies described in this paper is to improve the performance of this kind of heating system by creating more uniform temperature distribution in the environment around the reflector.

Hartwig [6] studied steady state heat transfer measurement. He installed measuring devices in hollow ceramic and metal cylinders and measured heat flow inside the cylinders under different combinations of pressure and temperature.

Hojer et al. [7] attempted to measure the effect and influence of the shape of the burner of an overhead luminous infrared heater on the ambient heat distribution. They compared the mathematical and experimental results to show that the shape of the burner was more significant than the geometry of the reflector in determining radiant heat transfer from the luminous heater.

Beker and Laurien [8 and 9] studied heat transfer in a high temperature reactor. They focused on finding factors that influence temperature distribution in a high temperature reactor using CFX-4 code for computation and simulations. The interior layer of a reactor was used as a heat and temperature reflector [10].

In this paper, we build a computer model using the principles of computational fluid dynamics (CFD) in order to investigate the effects of reflector shape on temperature distribution and power consumption.

We performed the following tasks to optimise the Kanthal Superthal high power reflector:

1- Six different shaped reflectors were simulated under the same input boundary and initial conditions.

2- A three dimensional simulation was performed to support and verify the two dimensional results.

3- An optimum configuration was suggested based on the evaluation of these results.

Figure 1. A Kanthal Superthal high power reflector[1].

Table 1. Specifications of the Kanthal Superthal high power reflector[2].

Width	700mm	Voltage	66V at 1650 °C
Height	700mm	Current	605A at 1650 °C
Depth	350mm	Power density	110kW/m^2
Power	40kW	Element Temperature	Up to 1650 °C
Element type: Kanthal Super special, 12/24			

II. SIMULATION

Simulations were performed in COMSOL software [12] by producing the correct geometry and applying suitable boundary conditions. Most simulations were done with a two dimensional model, and were subsequently supported by results from a three dimensional model.

[1] From Kanthal product sheet
[2] From Kanthal product sheet

A. 2D simulation setup

The simulation was performed in the COMSOL environment [12]. Three different hood geometries were investigated. The hoods are named based on their shape: rectangular, circular and angled reflectors and are shown in Figure 2. Right sides describe the dimensions and left ones of figure 2 shown the boundary conditions of element and hoods. They have a circular cross section in the horizontal plane. The diameter of the opening at its widest point is the same in each case. In the simulation, all the material and fluid properties, including thermal conductivity, density and specific heat capacity for air and reflector materials are considered as being dependent on temperature and this is set in the software.

The thickness of the insulating fibre is a constant 100 mm in the walls and bottom of each hood.

The boundary conditions of the simulation are described below.

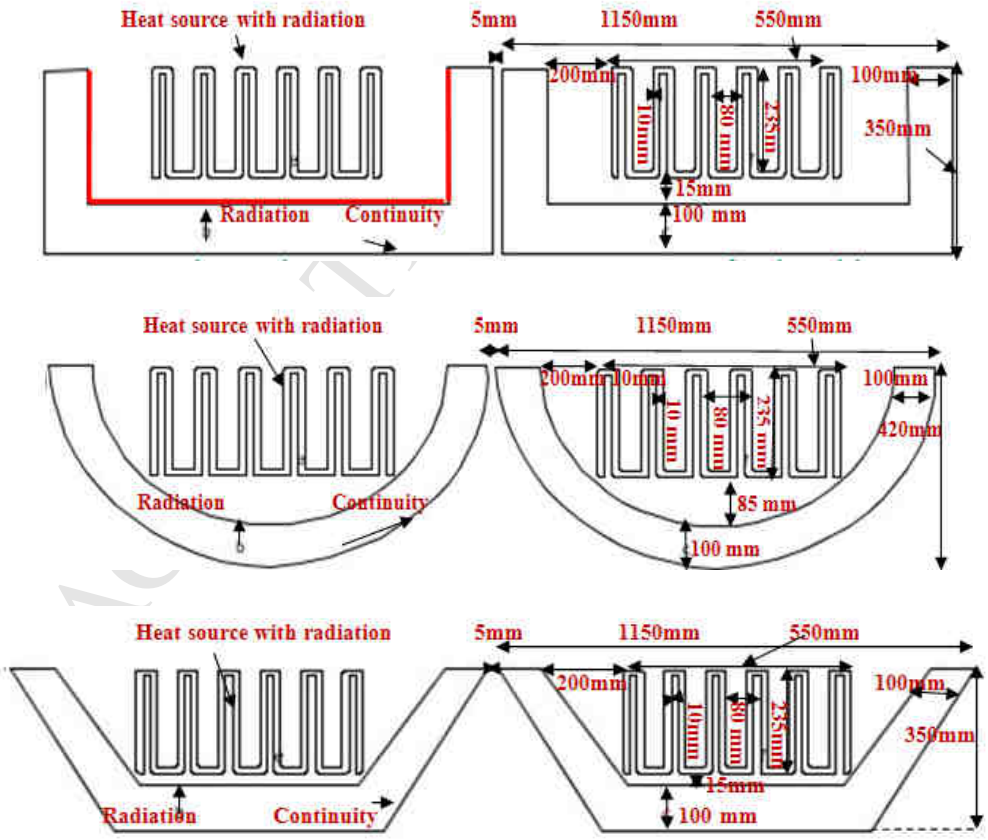

Figure 2. Schematics of the reflectors used in the simulations.

The element is given a constant power of 50 W/cm^2 in all two dimensional simulations. This is calculated as P/(D*L). Where D is the element diameter (10 mm), L is the total length of the element (approximately 34×L_e where L_e is the height of each sub-element, which is 235 mm) and P is the power, which is 40 kW. Emissivities are 0.7 for the element and 0.3 for the reflector. The radiosity of the reflector is therefore $0.3\times5.67\cdot10^{-8}\cdot T^4$ [W/m^2 K^4]. The radiosity of the element is $0.7\times5.67\cdot10^{-8}\cdot T^4$ [W/m^2 K^4]. The ambient air temperature is assumed to be a constant 300 K. The heat transfer coefficient (HTC) is set at 100 W/m^2 K for both element and hood. This value is calculated with the formulae presented by Januszkiewicz [13]:

$$\text{HTC} = 1.283 \times \sqrt{T_{hood} - T_{ambient}} + \varepsilon\sigma \frac{T_{hood}^4 - T_{ambient}^4}{T_{hood} - T_{ambient}}$$

The hood temperature is calculated numerically using the conventional equation and was found to be 1400K. These equations of conduction, radiation and convection equations that mentioned are found in the next paragraphs, heat transfer books and COMSOL software package as well.

III. GOVERNING EQUATIONS

Heat transfer by conduction is modelled as a mathematical formulation in the form of the heat equation [14 and 15]:

$$\rho C \frac{\partial T}{\partial t} + \nabla \cdot (- k\nabla T) = Q \qquad \textbf{(1)}$$

Where T is the temperature, ρ is the density, C is the heat capacity, k is the thermal conductivity, and Q is a heat source or heat sink.

In the steady state, the temperature does not change with time, and the first term containing ρ and C does not contribute to the simulation [12 and 14].

The heat equation also includes a convective term to take into account fluid conduction and convection. In terms of the general heat transfer model, this can be defined as:

$$\rho C_p \frac{\partial T}{\partial t} + \nabla \cdot (- k\nabla T + \rho C_p Tu) = Q \quad \textbf{(2)}$$

Where *Cp* is the heat capacity at a constant pressure, and *u* is the velocity field, which can either be provided as a mathematical expression of the independent variables or calculated by coupling to a momentum balance application mode such as incompressible Navier-Stokes or non-isothermal flow. The parenthesised term in Equation (2) represents the heat flux vector. This equation can be rewritten as Equation (3) for transfer through conduction and convection:

$$q = -k\nabla T + \rho C_p Tu \quad \textbf{(3)}$$

Where *q* is the heat flux vector. When heat transfer occurs by conduction only, *q* is given by:

$$q = -k\nabla T \quad \textbf{(4)}$$

A. Boundary Conditions

Two different types of boundary conditions, the Dirichlet type and the Neumann type are used for hoods. In addition, the heat source boundary condition is added to element surfaces. The Dirichlet type boundary condition is used to set the temperature on the hood boundary:

$$T = T_0 \quad \textbf{(5)}$$

While the Neumann type condition is used to set the heat flux on the boundary:

$$-n \cdot q = q_0 \quad \textbf{(6)}$$

Where *q* is the heat flux vector, *n* vector normal to the boundary, and q_0 is inward heat flux normal to the boundary.

The heat transfer module in COMSOL uses the following more general formulation of Equation (6) that includes convection:

$$-n \cdot q = q_0 + h(T_{\text{inf}} - T) \quad \textbf{(7)}$$

This accounts for the heat flux in terms of a constant heat flux q_0 and an ambient temperature (T_{inf}) dependent term that includes the HTC *h*.

q_0 is set to zero at symmetry boundaries.

B. Radiative Heat Transfer

Heat transfer by radiation is the third mechanism of heat transfer, and is considered for higher temperature elements. It is caused by the temperature dependent flux of electromagnetic waves that is emitted by a body, also known as thermal radiation.

Additional terms are required to represent the radiative heat flux. The net radiative heat flux q in the inward direction can be described as

$$q = \varepsilon(G - \sigma T^4) \quad \textbf{(8)}$$

Where G is the irradiation term and σ is the Boltzmann constant, $5.67 \cdot 10^{-8}$ [W/m^{2}K^4].

There are two types of radiative heat transfer: surface-to-ambient radiation and surface-to-surface radiation. These are distinguished by the respective boundary conditions. Equation (8) is general and applies to both radiation types. However, the irradiation term G differs for each type.

The following assumptions apply to surface-to-ambient radiation:

- A constant temperature T_{amb} is assumed for ambient surroundings with respect to the surface.
- The surroundings are assumed to behave as a black body, i.e. emissivity and absorptivity are equal to 1 and reflectivity is zero.

Following these assumptions, the irradiation term becomes

$$G = \sigma T_{amb}^4 \quad \textbf{(9)}$$

The net inward heat flux for surface-to-ambient radiation is therefore obtained by substituting Equation (9) into Equation (8):

$$q = \varepsilon\sigma(T_{amb}^4 - T^4) \quad \textbf{(10)}$$

This heat flux is added on the right side of Equation (7 **(7**) for boundaries where there is surface-to-ambient radiation.

The HTC is temperature dependent. To include HTC in the model, the following formula is used for boundary conditions:

$$-n_u.(k_u \nabla T_u) - n_d.(k_d \nabla T_d) = q_0 + h(T_{\text{inf}} - T) + \varepsilon\sigma(T_{amb}^4 - T^4) \quad \textbf{(11)}$$

Where u refers to the upper side and d refers to the lower side of the object (which happen to be equal in this model), n is the normal vector, T is temperature in K, k is thermal conductivity, q_0 is heat source in W/m^2, h is the HTC in $W/m^2.K$ and T_{inf} is the ambient temperature.

The conditions are more complicated in the case of surface-to-surface radiation. In the general case, the irradiation at a given point on the surface is determined by the geometry and local temperatures of the surrounding boundaries and the ambient temperature.

The total irradiation of the surface is therefore the integration of the heat flux from all points on the surface S´ plus the contribution of the ambient temperature. This is expressed as:

$$G_m = \int_{s'} \frac{(-\overline{n'}.\overline{r})(\overline{n}.\overline{r})}{\pi\left|\overline{r}\right|^4} J'ds + F_{amb}.\sigma.T_{amb}^4 \quad \textbf{(12)}$$

Where the integral over S' is the surface integral, J' is the radiosity (total outgoing radiative flux), G is the total incoming radiative flux , G_m is the mutual irradiation from other surfaces in the modelled geometry and F_{amb} is the view factor for the ambient surroundings.

The radiosity is defined as follows:

$$J = (1-\varepsilon)G + \varepsilon\sigma T^4 \quad \textbf{(13)}$$

G is substituted into Equation (12) to give Equation (13) for the radiosity:

$$J = \gamma\left\{G_m + F_{amb}.\sigma T^4\right\} + \varepsilon\sigma T^4 \quad \textbf{(14)}$$

Where ε is emissivity and γ= 1- ε. This equation is used to calculate the radiosity J at a surface point in 3D.

The dependent variable J is used on boundaries that participate in surface-to-surface radiation heat transfer.

IV. Results and Discussion

A. 2D Simulation results

Simulations were performed using the rectangular, angled and circular models. The horizontal temperature distributions 20 cm above the reflector surfaces that were calculated by each model were compared.

The results are shown in Figure 3 and Table 2. The angled shaped hood produces the highest maximum temperature, while the rectangular shaped hood results in a maximum temperature that is approximately 4 degrees lower. The circular hood produced a more uniform temperature distribution than the others.

The temperature is higher in the middle section for all the shapes. This is because of the higher heat losses at the sides compared to the middle.

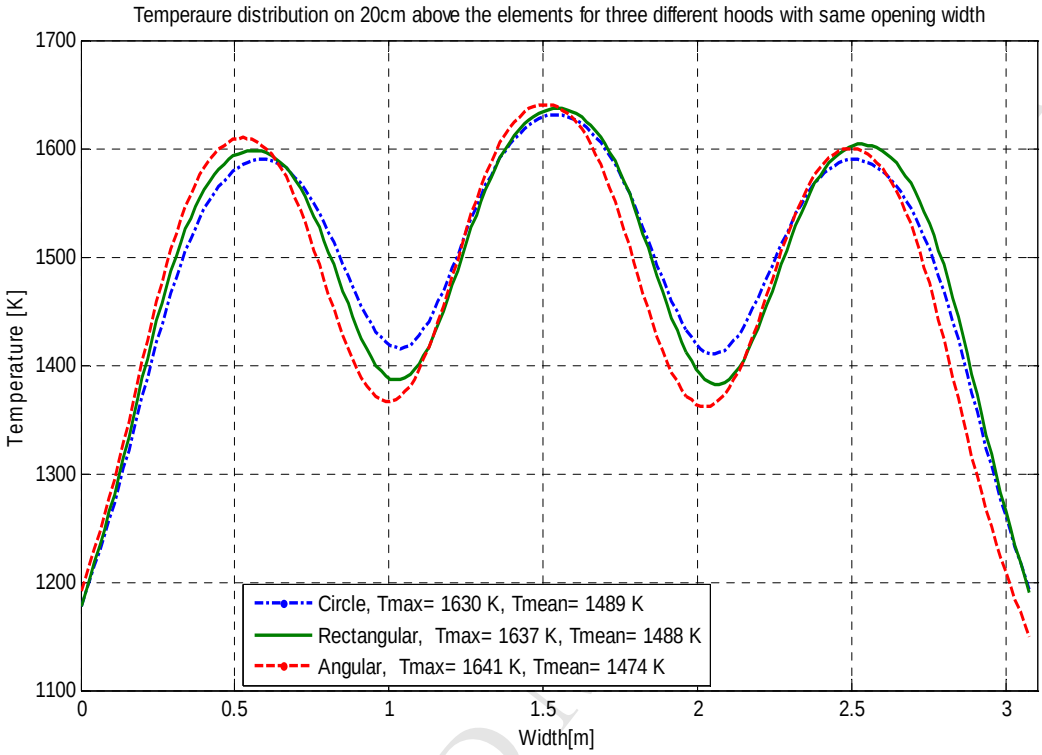

Figure 3. Comparison of the horizontal temperature distribution 20 cm above the reflector for different hood shapes.

Table 2. Simulation results 20 cm above the reflector.

Reflector shape	Mean Temperature	Maximum Temperature
Circle	1489 K	1630 K
Angled	1474 K	1641 K
Rectangular	1488 K	1637 K

The vertical temperature distributions, from the bottom of the hood to 80 cm above the reflector surface were also compared. These results are shown in Figure 4. It can be seen that the angled shaped

hood gives a higher temperature throughout the domain, while there is a larger temperature drop with distance from the hood for the rectangular hood.

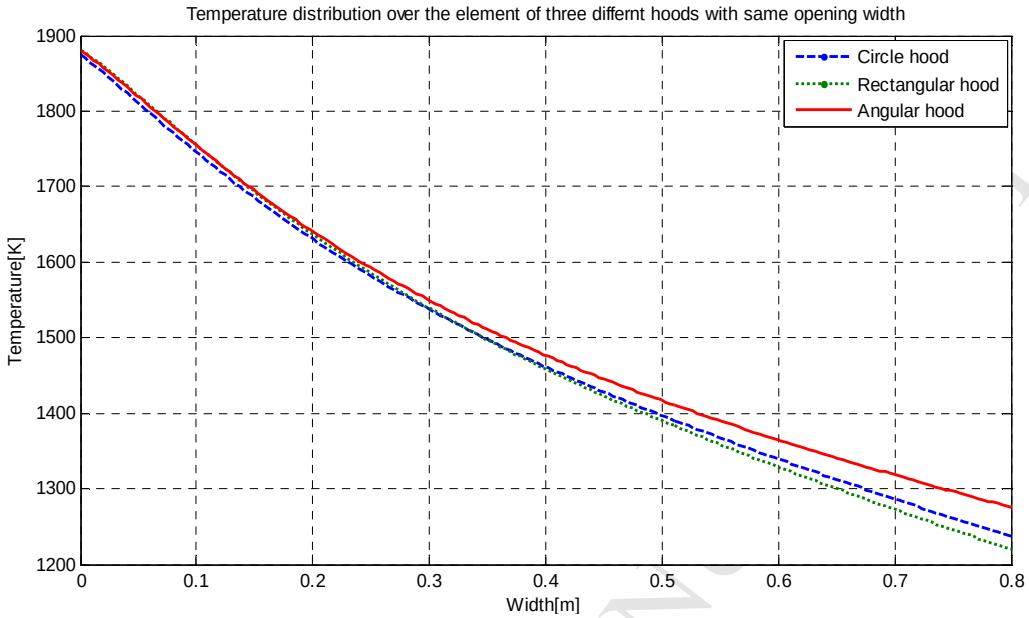

Figure 4. Comparison of temperature drop with distance from element for three different hood shapes.

It should be noted that temperature differences between the different reflectors increase with the vertical distance. For example the difference in temperature between the angled and circular hoods is around 1% at 20 cm from the reflector, and 4% at 80cm.

Figure 3 shows that the reflector shape does not have a large effect on the maximum temperature.

The slightly higher temperature for the angled form is a result of the smaller losses due to there being a smaller surface area that is exposed to the cooler ambient temperature at the rear of the reflector.

From the results of these simulations, and considering the fact that a rectangular shaped fibre hood is easier to manufacture, the rectangular shaped hood might be regarded as the preferred choice for real world applications.

To define mathematical formulae to describe of height effects on temperature, three order formulae that have the best fit show in equation 15.

The temperature distribution over the reflectors is given by the general formula:

$$T(x)= P_1*x^3 + P_2*x^2 +P_3*x^1 + P_4 \quad \textbf{(15)}$$

This formula generated from the simulation results as well as figure 4, with using of MATLAB software package calculated it. The constants are shown in Table 3.

Figures 5 to 7 show the simulated temperature distributions in the entire domain for each reflector shape (circular, rectangular and angled).

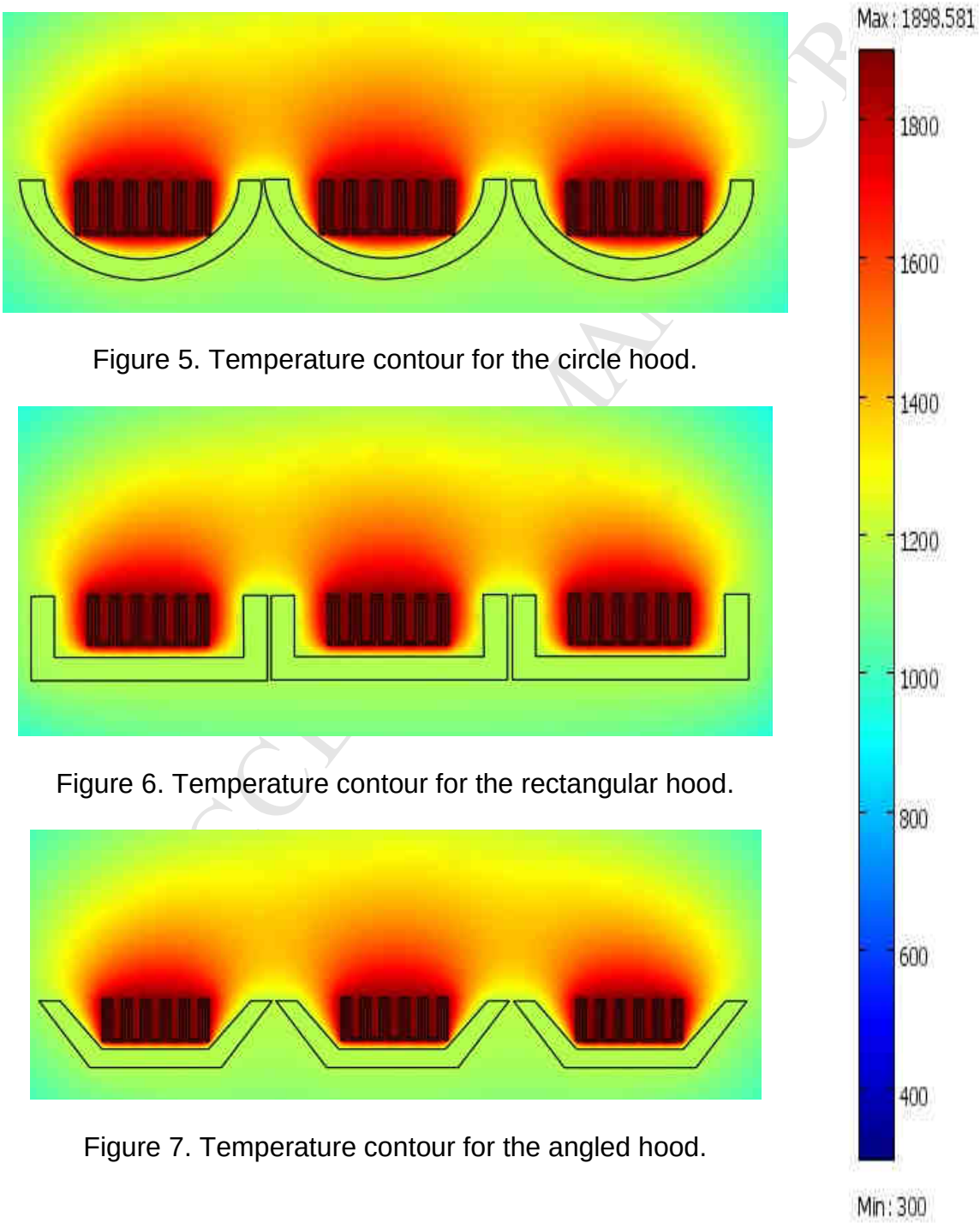

Figure 5. Temperature contour for the circle hood.

Figure 6. Temperature contour for the rectangular hood.

Figure 7. Temperature contour for the angled hood.

Table 3. Temperature distribution formulae coefficients (Equation 15).

Reflector shape	P_1	P_2	P_3	P_4
Circle	-646.75	1380.4	-1497.6	1880.7
Rectangular	-558.7	1271.5	-1498.6	1890.5
Angled	-629.92	1411.3	-1493.1	1888.5

B. Simulation with varying opening width

The following simulations look into the effect of the width of the reflector opening on the temperature profile and distribution. A comparison is made between three angled reflectors and two rectangular reflectors.

Figure 8 shows the horizontal temperature distributions above the reflectors, in cross side (Figure 8 a) and vertical side (Figure 8b). It shows that the angled reflector with a 1150 mm opening produces the highest maximum temperature. However, the angled reflector with the smallest (900 mm) opening produces a more uniform temperature distribution. The smaller opening would therefore be preferred in applications that require more uniform temperatures. See table 4 for more information..

The angled hood with the smallest opening also produces the highest mean temperature over the horizontal area, approximately 28 degrees higher than that produced by the 1150 mm opening. The vertical temperature distribution above the reflectors is largely unaffected by the size of the opening.

From the results in the previous section, it was apparent that the shape of the reflector did not have a large effect on the temperature distribution. However, the size of the opening affects the mean temperature, and therefore the efficiency, but does not have a large effect on the maximum temperature.

An increase of the diameter of the opening of the angled reflector from 900 mm to 1150 mm, or about 21.7%, increased the maximum temperature 20 cm above the element by 0.67%, but reduced the mean temperature by 1.9%.

Figure 9 shows the results of using a rectangular reflector, in cross side (Figure 9 a) and vertical profile in height (Figure 9b). Increasing the width of the opening of the rectangular reflector from 820 mm to 1150 mm increases both mean and maximum temperatures 20 cm above the reflector. The temperatures are therefore dependent on the width of the opening, but if the width remains the same, changing the shape of the reflector does not affect the temperature distribution much. As with the angled reflectors, the effect of the width of the opening on the mean temperature is much larger than the effect on the maximum temperature.

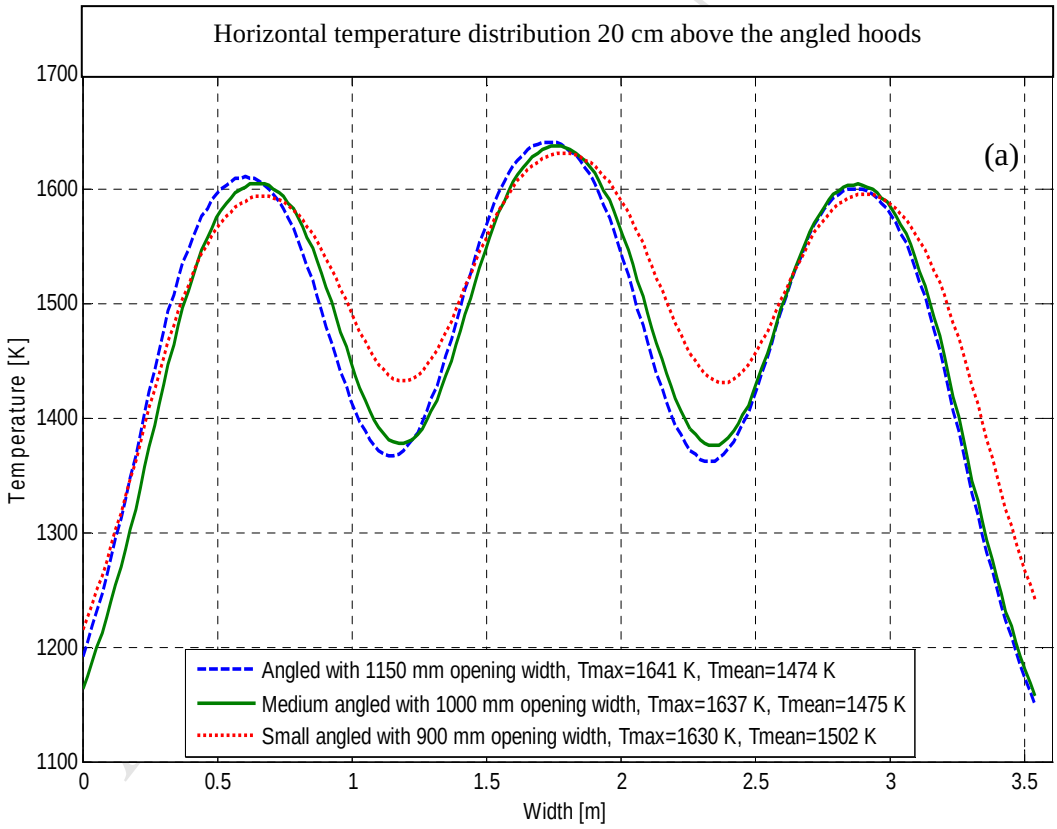

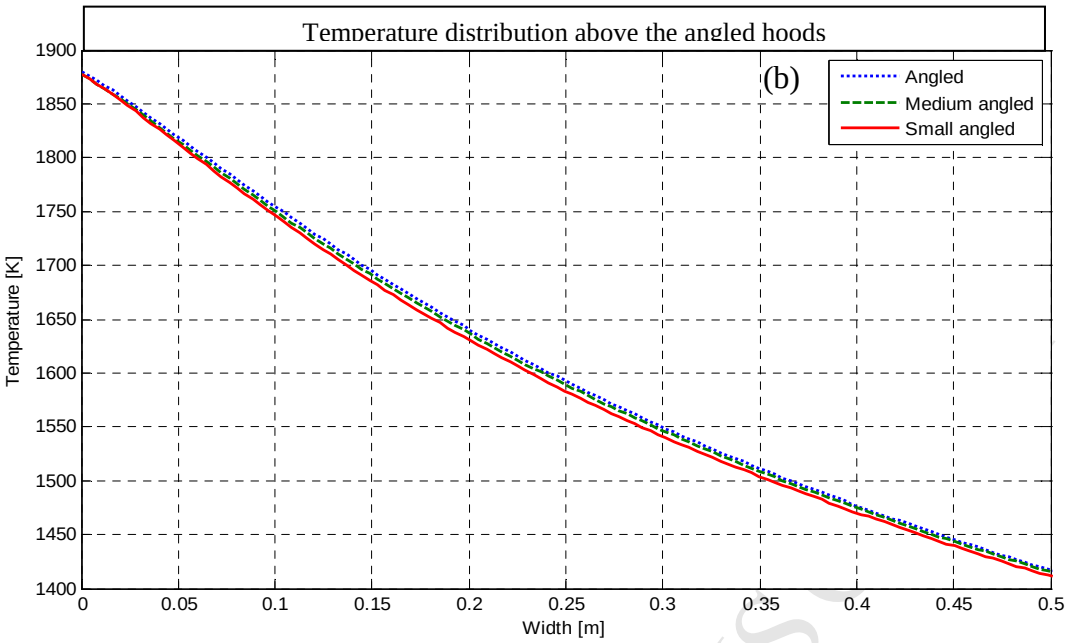

Figure 8. Comparison of the temperature distributions for angled hoods with different opening widths.

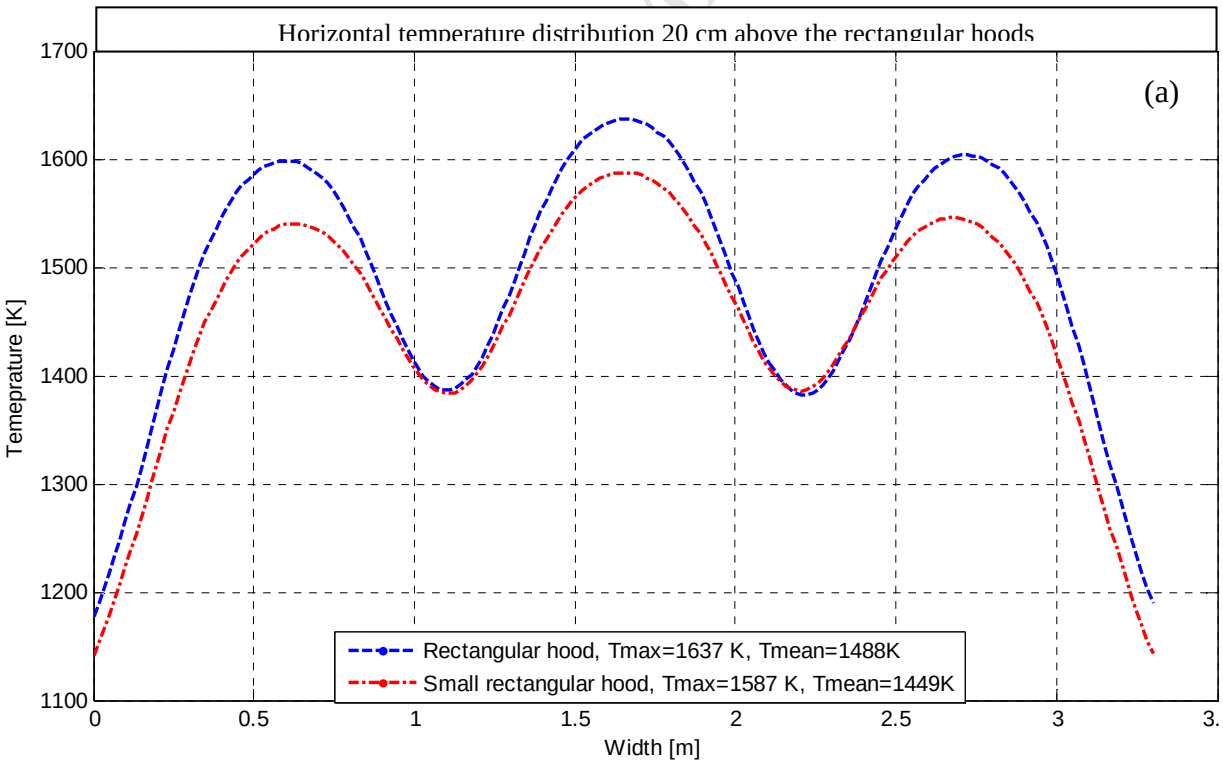

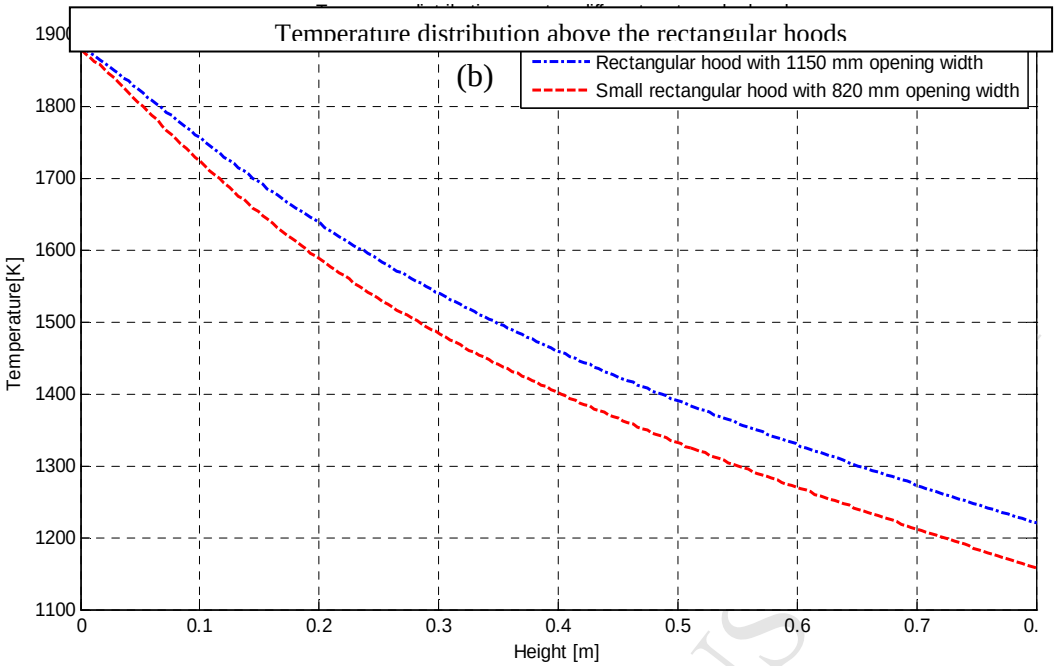

Figure 9. Comparison of the vertical temperature distribution for rectangular hoods with different opening widths.

Accurate formulae with at least 3 degree polynomial (like equation 14 for Figure 9 b) were derived from the simulation, see Table 5 for coefficients.

These formulae were obtained by using CFD calculations of temperature distribution by the finite element method, with using of COMSOL and Matlab packages.

Table 4. Simulation results of temperatures 20 cm above the reflector.

Reflector shape	Mean Temperature	Maximum Temperature
Small angled	1502 K	1630 K
Medium angled	1475 K	1637 K
Angled	1474 K	1641 K

Table 5. Temperature distribution coefficients above the reflector (Equation 15).

Reflector shape	P_1	P_2	P_3	P_4
Angled	-629.92	1411.3	-1493.1	1888.5
Medium angled	-664.03	1451.3	-1500.8	1884.9
Small angled	-783.86	1592.8	-1548.9	1884.2

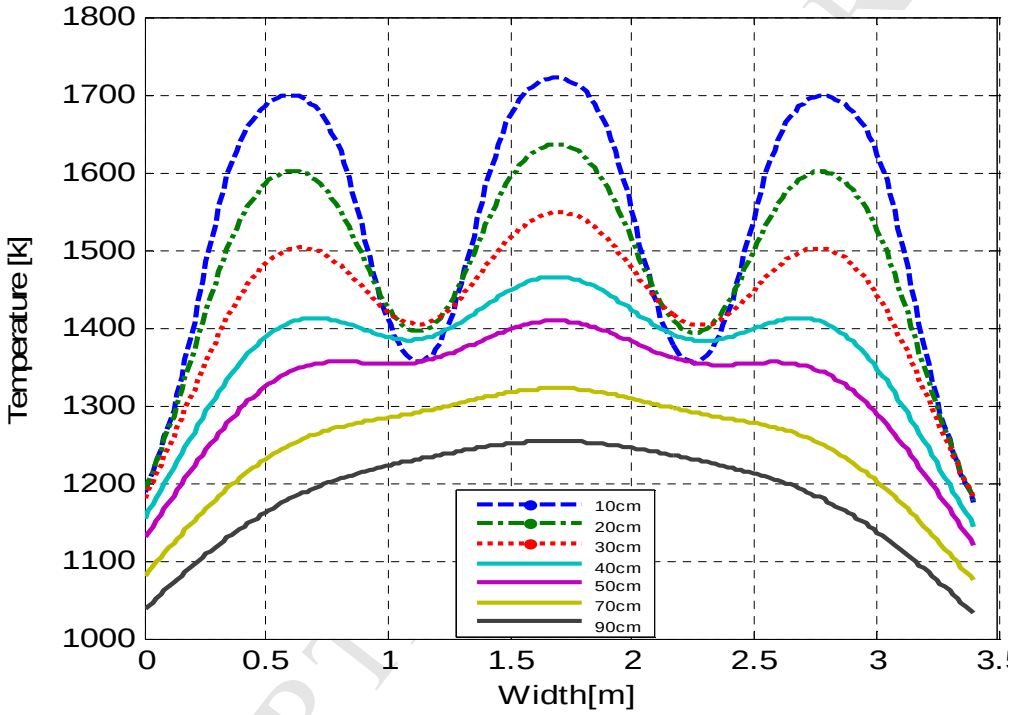

Figure 10. Temperature profiles for the small angled hood model at different heights above the reflector.

It is often desirable to produce a homogeneous temperature distribution over a large area. In order to determine the optimum distance between the heater and the heated object, the temperature distribution at different distances from the reflector was plotted (Figure 10). A flat temperature profile was obtained between 40 and 70 cm above the reflector.

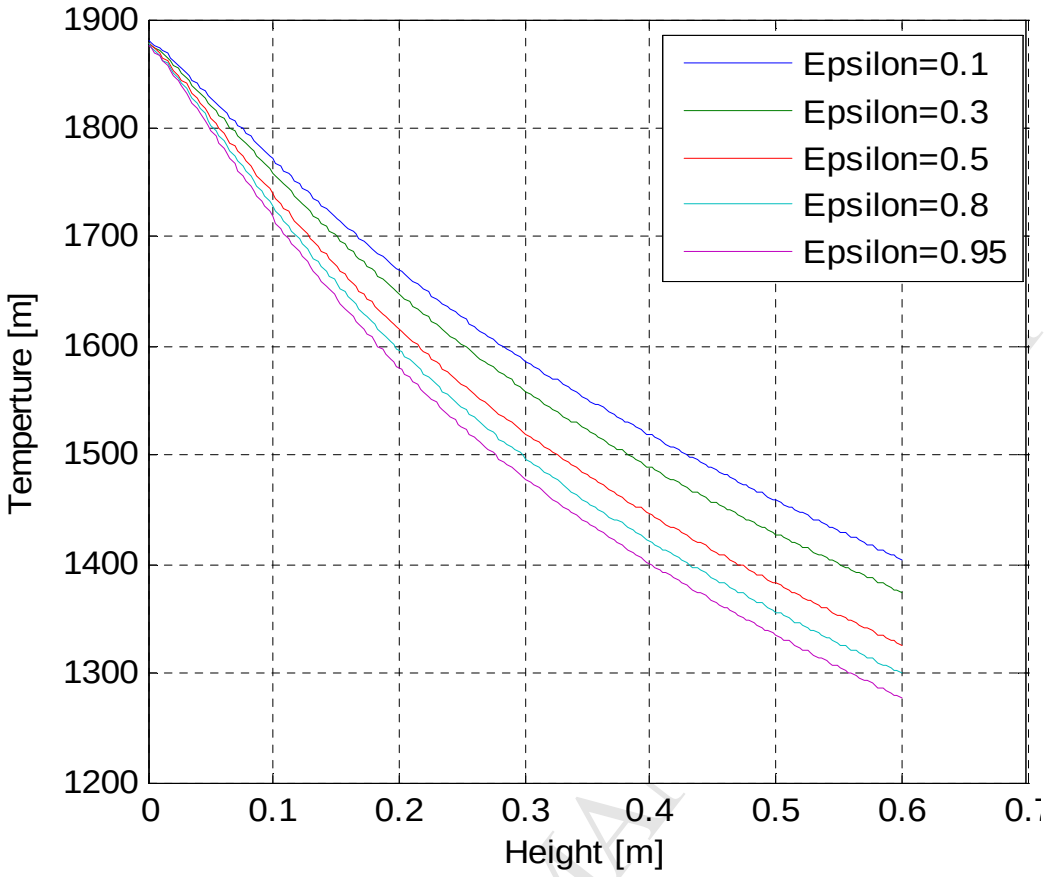

Figure 11. Effect of varying emissivity on the element temperature [K].

The influence of emissivity is shown in Figure 11. The emissivity of the angled reflector was varied from 0.1 to 0.95, and the variation of temperature with height above the reflector was plotted.

Figures 12 to 14 show the simulated temperature distributions in the entire domain for each reflector shape (in contour profiles for small and medium dngled and for small rectangular). These figures show a clear views rather than to last curves to readers.

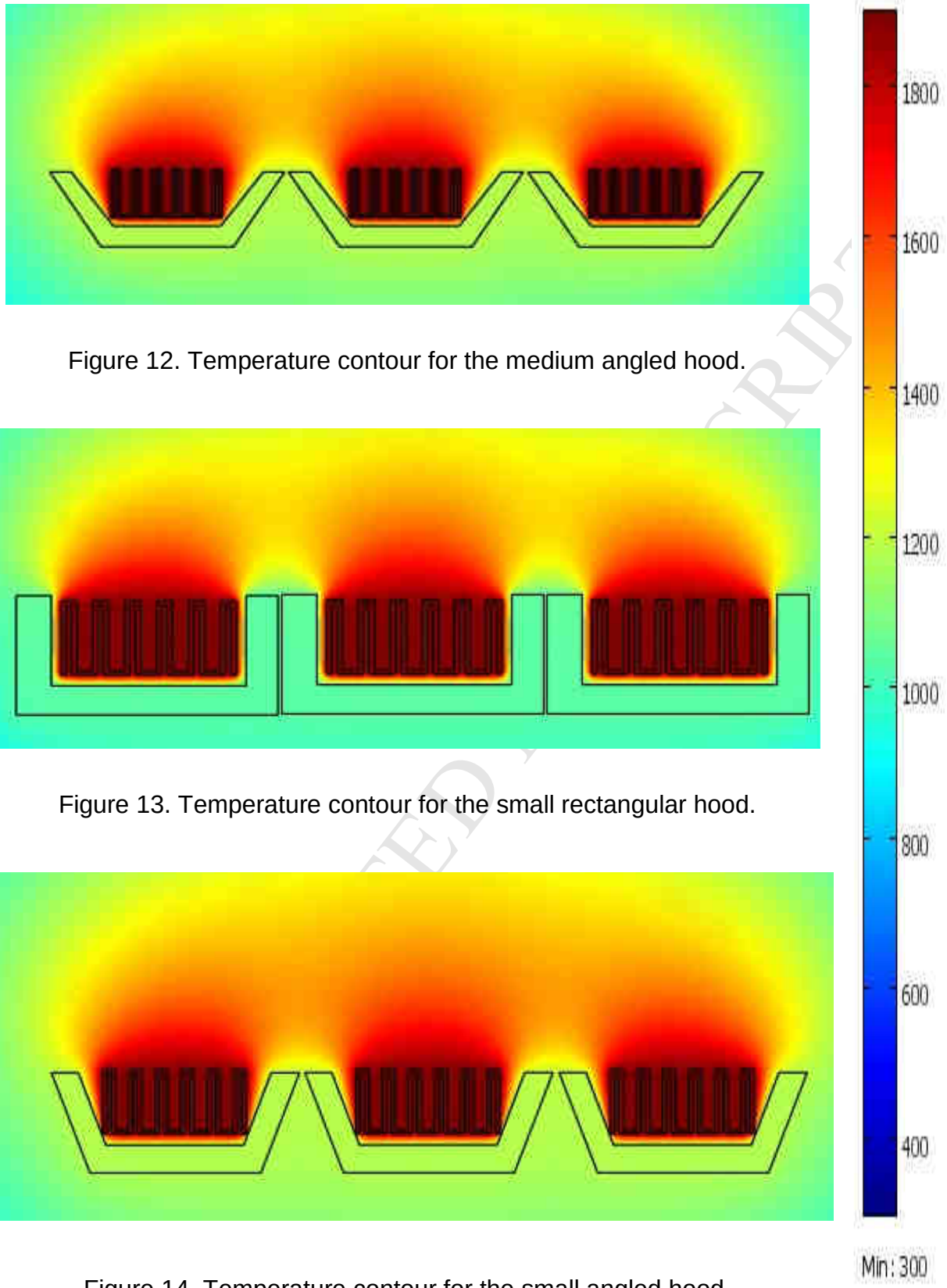

Figure 12. Temperature contour for the medium angled hood.

Figure 13. Temperature contour for the small rectangular hood.

Figure 14. Temperature contour for the small angled hood.

C. 3D simulation results

A simplified conical reflector was simulated in three dimensions. The results of this simulation are shown in Figures 15 and 16. The dimensions of this model are the same as for the small angled model i.e. a height of 350 mm, a fibre thickness of 100 mm and a 900 mm opening diameter. The boundary conditions for this simulation were the same as for the 2D models. The temperature profile and temperature distribution showed good resemblance and similarity with the 2D models. This comparison is shown in Figure 17.

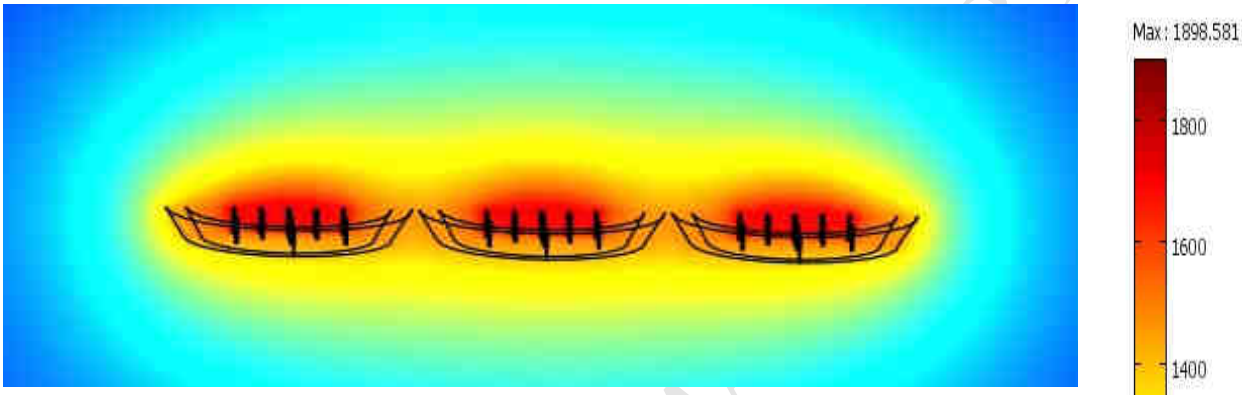

Figure 15. Temperature contour for conical hood in 3D.

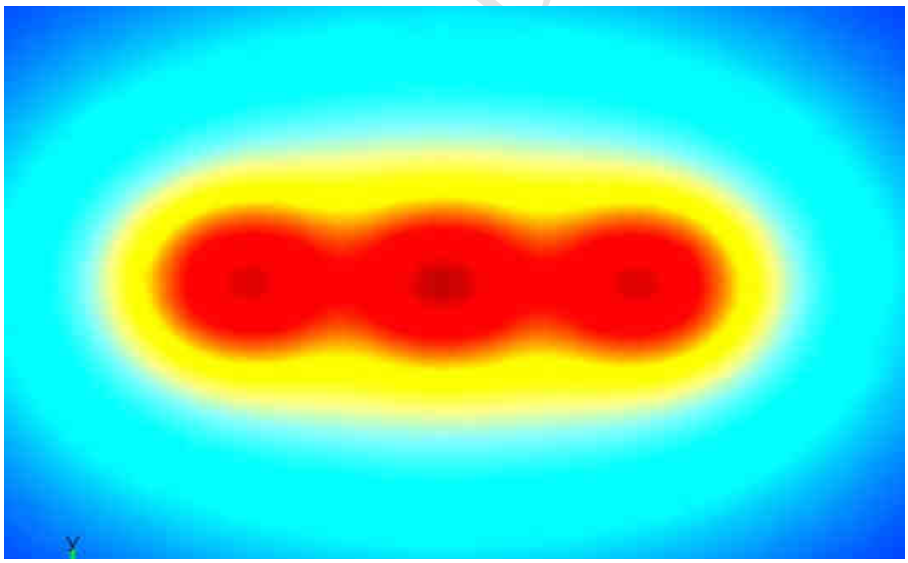

Figure 16. Temperature contour for conical hood 20 cm above the element.

Based on this figure the difference between the 2D and 3D models is about 5%. The temperature difference increases with increasing height above the element, from around 0.47% on the reflector (this difference is within the limits of numerical errors) to around 5% at 20 cm above the element.

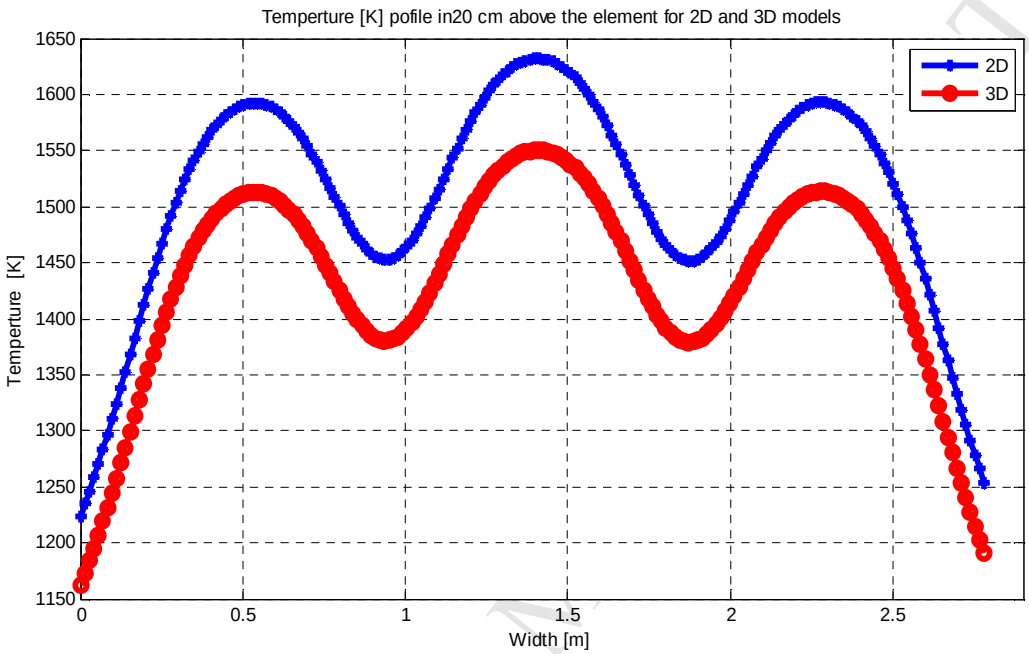

Figure 17. Comparison of temperature profiles 20 cm above hoods generated by simulations using 2D and 3D models.

The data from the comparison of the 2D and 3D temperature curves in Figure 17 are shown in Table 6.

Table 6. Temperature comparisons for 2D and 3D simulations.

Description	Temperature[K] for 2D	Temperature[K] for 3D	Difference %
Min temperature	1224	1162	5%
Max temperature	1630	1537	5.8%
Mean temperature	1502	1434	4.97%
Median temperature	1529	1453	4.97%

The reflector temperature is the same in both models because the same boundary conditions were used in each case. Equation 16 was used to determine the temperature differences between the 2D and 3D models:

$$(|(T_{}2D - T_{}3D)/T_{}2D\,| \times 100) \quad \textbf{(16)}$$

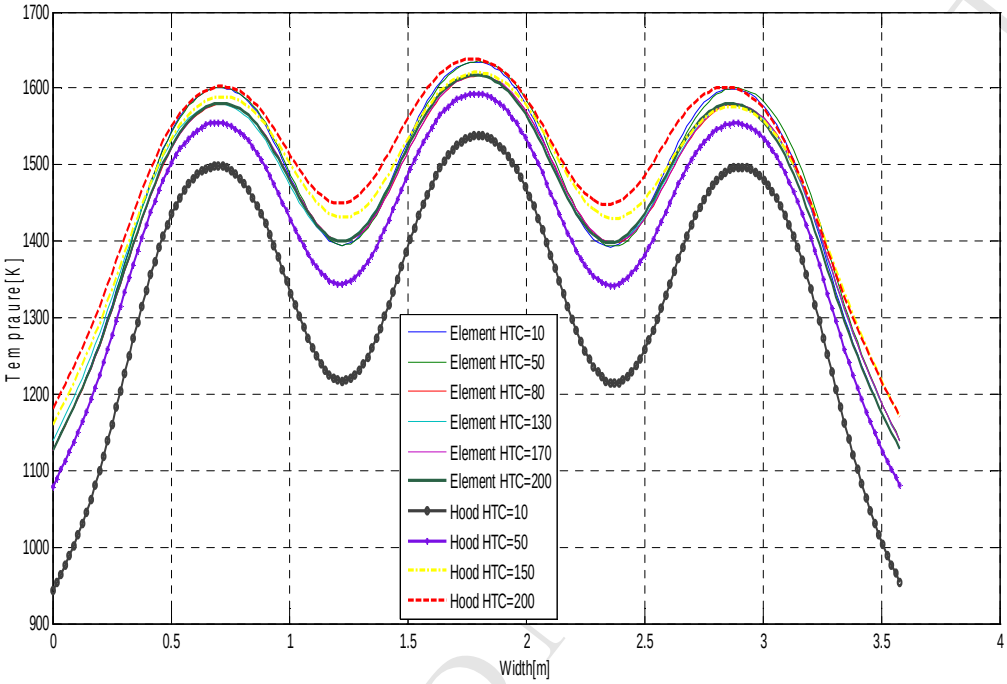

Figure 18. Effect of HTC on temperature 20cm above the hood.

The HTC is temperature dependent. In order to investigate the effect of the HTC on the temperature distribution, simulations were performed with different HTC values for both hood and element with the small angled hood model. Equation 14 was used to include the effects of HTC on the temperature distributions, and also to define the boundary conditions of the hood and element. The HTC of the hood was fixed at 100 W/m^{2}K while the HTC of the element was varied, and vice versa. The results of these simulations, are shown in Figure 18, and indicate that varying the HTC of the hood has a considerable effect on the temperature profile. The temperature profile is less sensitive to variations in the HTC of the element.

V. CONCLUSIONS

The simulations performed here show that the shape of the reflector hood does not have a large effect on temperature profiles above the reflector. Angled reflectors produce the highest maximum temperatures above the reflector. A high mean temperature with little variation is highly desirable in furnaces. Reducing the diameter of the opening of the angled reflector produces the highest mean temperature. The temperature profile flattens out as we move away from the reflector and is almost flat on a surface 50 cm above the reflectors.

The simulations also showed that 2D models give reasonably accurate results. A comparison between 2D and 3D models showed only a 5% difference.

Consequently, according to simulation results, the optimum reflector has an angled shape (to produce the maximum temperature), with a small opening (to produce a more uniform and higher mean temperature). Also, due to lower fiber surface of rectangular, it can be an alternative to use in this system.

This work has been driven by the demand to optimise the high power reflectors in ferromagnetic strip annealing furnaces to produce uniform temperatures at a predefined distance. These can replace the gas fired burners that are commonly used.

Simulation results showed that uniform temperatures can be achieved at distances of more than 50 cm from the reflector. Uniform temperatures result in better control of size and shape of grains in the ferromagnetic strips.

VI. REFERENCES

[1] www.kanthal.com, September, 2010

[2] http://www.isquaredrelement.com/ , September, 2010

[3] http://www.rotfil.com/en/index.asp, September, 2010

[4] http://www.duralite.com/, September, 2010

[5] Kanthal AB product sheet, www.kanthal.com, September, 2010

[6] Frederic W. Hartwig, 1957, Development and application of a technique for steady state aerodynamic heat transfer measurements, Pasadena, California institute of technology, doctoral thesis.

[7] Ondrej Hojer et al., 2000, On the relation between shape and downward radiation of overhead radiant heaters, 8th European Conference on Industrial Furnaces and Boilers.

[8] S. Becker and E. Laurien, 2002, Three dimensional numerical simulations of flow and heat transport in a high temperature reactor, IAEA, www.iaea.or.at.

[9] Becker, S. and Laurien, E., 2001, Numerical simulation of the convective heat transport in pebble beds at high temperatures; Annual Meeting Nuclear Technology 2001, May 14-17,Dresden, Germany

[10] A. J. Heron and G. B. Schaffer, 2003, Mechanical alloying of MoSi2 with ternary alloying elements.: Part 1: Experimental , Materials Science and Engineering A Volume 352, Issues 1-2, Pages 105-111

[11] N. Zacchetti, K. Mizuno, 2004, Characterization of MoSi2 coatings obtained by atmospheric pressure and low-pressure plasma spraying, Surface and Interface Analysis, Volume 18 Issue 8, Pages 589 – 593, John Wiley & Sons, Ltd.

[12] COMSOL software, version 3.4, Stockholm, Sweden

[13] K. T. Januszkiewicz, 1999, Numerical model of the heating-up system with heating rods, Elsevier Journal, Advances in Engineering Software Volume 30, Issue 2, Pages 141-145

[14] Necati Özisk, M. 1985, Heat transfer: a basic approach, McGraw-Hill.

[15] Frank P. Incropera, David P. DeWitt Fundamentals of Heat and Mass Transfer, 5th Edition, Book